38. Onat A, Hergenc G, Uyarel H *et al*. Prevalence, incidence, predictors and outcome of type 2 diabetes in Turkey. *Anadolu Kardiyol Derg* 2006; 6: 314–321
39. Jones CA, Francis ME, Eberhardt MS *et al*. Microalbuminuria in the US population: Third National Health and Nutrition Examination Survey. *Am J Kidney Dis* 2002; 39: 445–459
40. Altun B, Arici M, Nergizoglu G *et al*. Prevalence, awareness, treatment and control of hypertension in Turkey (the PatenT study) in 2003. *J Hypertens* 2005; 23: 1817–1823
41. Arici M, Turgan C, Altun B *et al*. Hypertension incidence in Turkey (HinT): a population-based study. *J Hypertens* 2010; 28: 240–244
42. Ejerblad E, Fored CM, Lindblad P *et al*. Obesity and risk for chronic renal failure. *J Am Soc Nephrol* 2006; 17: 1695–1702
43. Kurella M, Lo JC, Chertow GM. Metabolic syndrome and the risk for chronic kidney disease among nondiabetic adults. *J Am Soc Nephrol* 2005; 16: 2134–2140
44. Oguz A, Temizhan A, Abaci A *et al*. Obesity and abdominal obesity; an alarming challenge for cardio-metabolic risk in Turkish adults. *Anadolu Kardiyol Derg* 2008; 8: 401–406
45. Sanisoglu SY, Oktenli C, Hasimi A *et al*. Prevalence of metabolic syndrome-related disorders in a large adult population in Turkey. *BMC Public Health* 2006; 6: 92
46. Kim S, Lim CS, Han DC *et al*. The prevalence of chronic kidney disease (CKD) and the associated factors to CKD in urban Korea: a population-based cross-sectional epidemiologic study. *J Korean Med Sci* 2009; 24: S11–S21
47. Nygaard H, Naik M, Ruths S *et al*. Clinically important renal impairment in various groups of old persons. *Scand J Prim Health Care* 2004; 22: 152–156

Received for publication: 14.5.10; Accepted in revised form: 1.10.10

Nephrol Dial Transplant (2011) 26: 1871–1881
doi: 10.1093/ndt/gfq604
Advance Access publication 5 October 2010

ADAMTS13—marker of contractile phenotype of arterial smooth muscle cells lost in benign nephrosclerosis

Clemens L. Bockmeyer[1,*], Vinzent Forstmeier[1,*], Friedrich Modde[1], Svjetlana Lovric[2], Ralf A. Claus[3], Mario Schiffer[2], Putri A. Agustian[1], Christina Grothusen[4], Karsten Grote[4], Ingvild Birschmann[5], Katharina Theophile[1], Hans H. Kreipe[1], Verena Bröcker[1] and Jan U. Becker[1]

[1]Institute of Pathology, [2]Clinic for Nephrology and Hypertension, Hannover Medical School, Hannover, Lower Saxony, Germany, [3]Department for Anaesthesiology and Intensive Care Therapy, Friedrich Schiller University Jena, Jena, Thuringia, Germany, [4]Department of Cardiology and Angiology and [5]Department of Hematology, Hemostasis, Oncology, and Stem Cell Transplantation, Hannover Medical School, Hannover, Lower Saxony, Germany

Correspondence and offprint requests to: Jan U. Becker; E-mail: JanBecker@gmx.com
[*]These authors contributed equally to this work.

Abstract

Background. Hypertensive nephrosclerosis alone and in combination with other renal diseases is a leading cause of terminal renal insufficiency. Histologic lesions manifest as benign nephrosclerosis (bN) with arteriolar hyalinosis and later fibrosis. Procoagulant micromilieus have been implicated in fibrosis. Hyalinosis is considered to consist of plasma insudation possibly containing procoagulant factors like von Willebrand factor (VWF). Therefore, it is hypothesized that VWF cleaving protease ADAMTS13 (a disintegrin-like and metalloprotease with thrombospondin type-1 motif, 13) is normally expressed by arteriolar vascular smooth muscle cells (VSMCs) and diminished in bN and that this reduction contributes to fibrosis in bN.

Methods. ADAMTS13 expression was examined by immunohistochemistry and quantitative real-time polymerase chain reaction in VSMCs of various human organs. Fifty-four specimens with and seven without bN were immunostained for ADAMTS13, VWF, CD61 and VSMC differentiation markers in arteriolar walls.

Results. Expression of ADAMTS13 is confirmed in VSMCs. In bN, ADAMTS13 immunostaining of arterial VSMCs correlated inversely with fibrotic but not hyalinotic lesions. Smooth muscle myosin heavy chain showed an inverse correlation with hyalinotic, as opposed to fibrotic lesions of bN. Smoothelin showed an inverse correlation with both hyalinotic and fibrotic lesions of bN. VWF was absent in normal controls and hyalinotic lesions, but present exclusively in fibrotic lesions in 7/54 (13%) bN cases. CD61 was absent in all arteriolar walls.

Conclusions. The present results establish ADAMTS13 as a novel marker of contractile VSMCs that is retained in early hyalinotic bN but partially lost later in fibrotic bN. Loss of ADAMTS13 and accumulation of VWF in fibrotic

but not hyalinotic arteriolar walls could further propagate fibrosis in bN.

Keywords: arterial hypertension; arterioles; hypertensive nephrosclerosis; kidney; sm-MHC

Introduction

Hypertensive renal disease is considered the second most common disease leading to end-stage renal failure in the USA [1], although it is argued that clinical data without biopsy verification overestimate the true prevalence [8]. Arterial hypertension is also an important progression factor in other renal diseases, notably diabetic nephropathy [7,12,13,30,38]. Benign nephrosclerosis (bN) is the most prevalent form of hypertensive damage in the kidney and often found in renal biopsies. Characteristic histomorphological findings in bN are hyalinosis, fibrosis and hypertrophy and kinking of preglomerular vessels. Hyalinosis is predominantly present in the media of the vessel walls [15]. This hyaline has been thought since the times of Fahr to consist of plasma insudation [11,15–17]. Hyalinosis has been described as potentially reversible and is considered to precede fibrosis [15]. Whereas hyalinosis only correlates with tubulointerstitial fibrosis and level and duration of arterial hypertension, fibrosis of small preglomerular vessels is considered the best correlate with glomerular and tubulointerstitial sclerosis, as well as renal function and level and duration of arterial hypertension [20].

Based mainly on studies in the liver, prothrombotic microenvironments have long been implicated in the development of fibrosis [3,50,52]. Among the proteins regulating the coagulation cascade that have been directly linked to the development of liver fibrosis is ADAMTS13 (a disintegrin-like and metalloprotease with thrombospondin type-1 motif, 13) [46], the cleaving protease of von Willebrand factor (VWF) multimers. The interaction of ADAMTS13 and VWF is one of the initial steps in haemostasis, and a lack of ADAMTS13 activity due to functionally relevant mutations [23,29,39] or inhibitory autoantibodies [10,44] causes thrombotic thrombocytopenic purpura. ADAMTS13 mRNA is detected in several organs, with the highest levels in the brain, liver, heart and placenta [32]. So far, *in vivo*, on a cellular level, ADAMTS13 expression has been described only in hepatic stellate cells [47,53], podocytes [26], tubular epithelial cells [27] and glomerular endothelial cells [26]. ADAMTS13 has also been detected in endothelial cells (ECs) *in vitro* [45].

Vascular smooth muscle cells (VSMCs) are closely related to hepatic stellate cells [51]. Therefore, we hypothesized that besides ECs, VSMCs might also express ADAMTS13 and that reduced levels of ADAMTS13 in VSMCs of small preglomerular vessels might contribute to a local prothrombotic, and thus profibrotic, microenvironment and promote the development of bN.

Materials and methods

Immunohistochemistry

In order to establish the expression of ADAMTS13 in VSMCs of normal arteries and arterioles of various human organs, formalin-fixed and paraffin-embedded (FFPE) tissue samples were examined by immunohistochemistry. Organ samples included brain, heart, lung, liver, spleen, pancreas, kidney, renal artery, placenta and also aorta (each $n = 3$, except for kidney $n = 7$). All were immunostained for ADAMTS13 using a polyclonal antibody directed against amino acids 1128–1427 of human ADAMTS13 (sc-25584, Santa Cruz Biotechnology, Santa Cruz, CA, USA) after epitope retrieval in Tris/EDTA at pH 9.0 for 20 min at 95°C. The bound primary antibody was visualized with diaminobenzidine (Zytomed Systems, Berlin, Germany) as a substrate for horseradish peroxidase (PolyHRP detection system, Zytomed Systems, Berlin, Germany). Staining was scored as absent, minimal, moderate or strong.

Paraffin sections were immunostained for activated platelets (CD61, C7280, Dako Cytomation, Hamburg, Germany), VWF (M0616, Dako Cytomation, Hamburg, Germany), alpha-smooth muscle actin (alpha-SMA) (M0851, Dako Cytomation, Hamburg, Germany), smooth muscle myosin heavy chain (sm-MHC) (M9850-16X, US-Biologicals, Swampcott, MA, USA) and smoothelin (clone 4A83, Abcam, Cambridge, UK). Pretreatment consisted of Protease XXIV digestion for CD61, Pronase (Sigma-Aldrich, Munich, Germany) digestion for VWF and incubation in citrate buffer pH 6.0 at 95°C for 20 min for sm-MHC and smoothelin. Staining was evaluated using the same scoring system as described for ADAMTS13.

For all immunostains, specificity of the primary antibodies was checked by incubation with irrelevant isotype controls (mouse IgG1, #DLN-05792, Dianova, Hamburg, Germany) for monoclonal antibodies (VWF, alpha-SMA, sm-MHC, CD61, smoothelin) and polyclonal rabbit IgG (#DLN-13124, Dianova, Hamburg, Germany) for the polyclonal ADAMTS13 antibody at equivalent concentrations.

Microdissection and quantitative real-time polymerase chain reaction

Expression of ADAMTS13 by VSMCs was confirmed on the mRNA level. TaqMan-based real-time polymerase chain reaction (RT-PCR) was performed after pre-amplification of microdissected VSMCs of normal renal arteries ($n = 3$) and umbilical veins ($n = 3$) as described recently

Table 1. Quantitative RT-PCR primers. ID # refers to the order number (all supplied by Applied Biosystems, Foster City, CA, USA)

Target transcript	TaqMan gene expression assay ID #
A disintegrin-like and metalloprotease with thrombospondin type-1 motif, 13 (ADAMTS13)	Hs00260148_m1
Smooth muscle myosin heavy chain (sm-MHC)	Hs00975778_m1
Alpha-smooth muscle actin (alpha-SMA)	Hs00909449_m1
Smoothelin	Hs00199489_m1
Polymerase II, RNA, subunit A (POLR2A)	Hs00172187_m1
Beta-glucuronidase (GUSB)	Hs99999908_m1

Table 2. Clinical data of the 55 patients with and 7 controls without benign nephrosclerosis (bN)

	Patients with bN ($n = 54$)	Controls without bN ($n = 7$)
Age (years)*	54 ± 15.3 ($n = 54$)	18 ± 8.6 ($n = 7$)
Systolic blood pressure (mm Hg)*	133 ± 27.2 ($n = 49$)	107 ± 14.7 ($n = 7$)
Diastolic blood pressure (mm Hg)*	78 ± 16.5 ($n = 49$)	66 ± 9.2 ($n = 7$)
Size (cm)	175 ± 9.6 ($n = 42$)	166 ± 30.9 ($n = 6$)
Body weight (kg)	83 ± 16.1 ($n = 43$)	68 ± 35.2 ($n = 6$)
Body mass index (kg/m^2)	27.3 ± 5.0 ($n = 41$)	22.8 ± 6.0 ($n = 6$)
Proteinuria*	21/30 (70%)	0/3 (0%)
Serum creatinine (μmol/L)*	180 ± 126.9 ($n = 47$)	80 ± 22.5 ($n = 6$)

*$P < 0.05$.

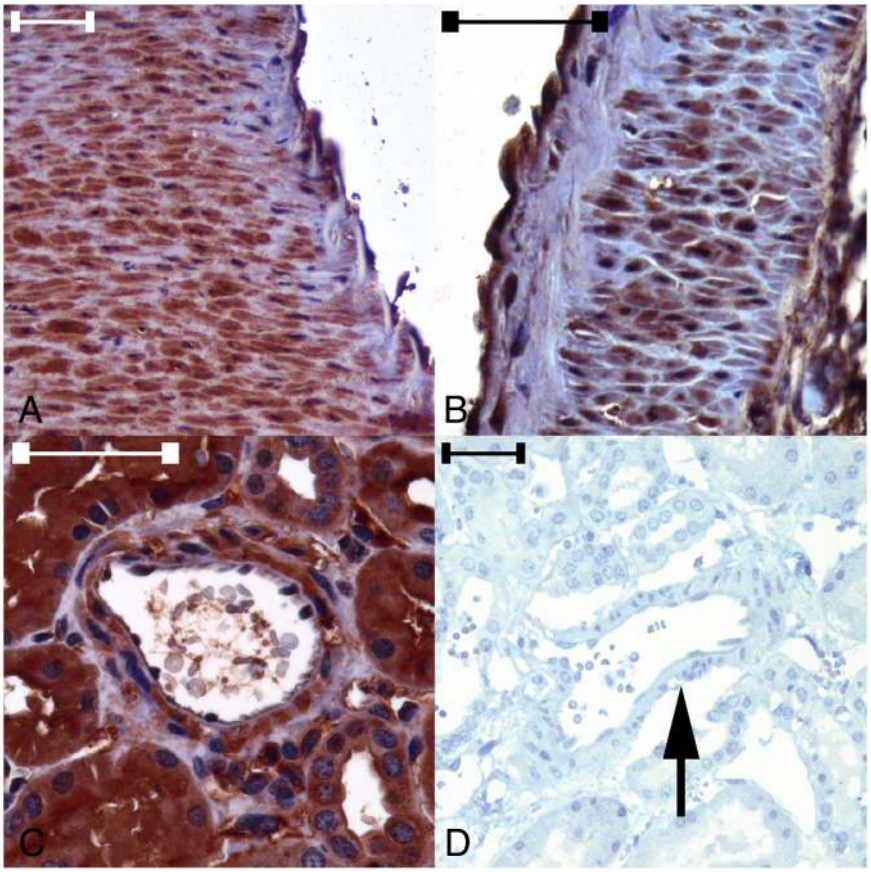

Fig. 1. ADAMTS13 immunostaining with moderate positivity (brown) VSMCs in the media of a renal artery (**A**), an arcuate artery (**B**) and an interlobular artery (**C**). Endothelial cells in A, B and C and tubular epithelial cells in C are also positive. Negative immunostaining of an interlobular artery (arrow) after incubation with irrelevant polyclonal rabbit IgG (**D**) as a control for ADAMTS13 antibody specificity. All immunoperoxidase, original magnification in A and D ×200, scale bar 50 μm. Original magnification in B and C ×400, scale bar 50 μm (B, C).

[42,43]. Desired cells were isolated from 5-μm sections of FFPE tissue with an MMI microdissector system (Olympus, Hamburg, Germany). RNA was isolated and transcribed into cDNA with the High Capacity cDNA Reverse Transcription Kit (Applied Biosystems, Foster City, CA, USA) and then pre-amplified. The primers shown in Table 1 (all Applied Biosystems, Foster City, CA, USA) were mixed with Gene Expression Mastermix (Applied Biosystems, Foster City, CA, USA). TaqMan RT-PCR runs were performed on the 7500 HT (Applied Biosystems, Foster City, CA, USA). For each sample, the ΔC_T was calculated as C_T target − (C_T POLRIIa + C_T GUSB) / 2, from which the relative expression was calculated as $2^{-\Delta CT}$.

Nuclease-free water was used instead of RNA samples as used as negative control [non-template control (NTC)] for cDNA synthesis.

Human kidney specimens

To examine the expression of ADAMTS13 in small preglomerular vessels with bN, 51 renal biopsies and tumour-free tissue from three renal cell carcinoma nephrectomies with an isolated diagnosis of bN and without any other vascular, glomerular or tubulointerstitial diseases (total n = 54) were selected from the archives of the Institute of Pathology of the Hannover Medical School. Seven histologically normal renal specimens from tumour nephrectomies (n = 6) and biopsies (n = 1) served as controls. The patients in this control cohort were significantly younger than the patients with bN ($P < 0.0001$, see Table 2). This could not be avoided since almost all older patients in our archives showed at least minimal bN.

Clinical data were gathered from the files of the respective clinic. Parameters included age, systolic and diastolic arterial blood pressure, body size, body weight, body mass index, proteinuria and serum creatinine.

All renal tissues were examined according to our standard protocol. Hyalinosis and fibrosis of small preglomerular vessels were assigned the following HScore (hyalinosis score) or FScore (fibrosis score): 0 (absent), 1 (minimal), 2 (moderate) and 3 (severe). The two scores were added together for a combined bN grading (bN-grade) defined as 0 (bN-grade absent), 1 to 2 (bN-grade minimal), 3 or 4 (bN-grade moderate) and 5 or 6 (bN-grade severe). In addition, all biopsies were evaluated for the total number of glomeruli, the frequency of globally sclerosed glomeruli and the presence and type of focal segmental glomerulosclerosis (FSGS) (perihilar, cellular, collapsing, tip lesion or not otherwise specified (NOS) as defined by D'Agati *et al.* [6]). The area ratio of cortical interstitial fibrosis and tubular atrophy (IFTA) to total cortical area was scored as IFTA 0 if <10%, IFTA 1 if <25%, IFTA 2 if <50% and IFTA 3 if ≥50%. ADAMTS13, VWF, alpha-SMA, sm-MHC and smoothelin immunostains were evaluated in small preglomerular vessels as defined by a muscular layer not more than three cells thick and again graded as absent, minimal, moderate or strong.

Statistical analysis and ethical approval

Statistical calculations were carried out with Statview (SAS Institute, Cary, NC, USA). For comparison of continuous variables, Mann–Whitney *U*-tests or Kruskal–Wallis tests were used, and for comparison of nominal variables, chi-squares of Fisher's exact tests were used. Results were considered as significant with $P < 0.05$.

All studies were conducted according to the Declaration of Helsinki [2] and were approved by the ethics committee of Hannover Medical School.

Results

ADAMTS13 expression in various human organs

ADAMTS13 immunohistochemistry. ADAMTS13 had a diffuse cytoplasmic staining pattern in all arterial VSMCs

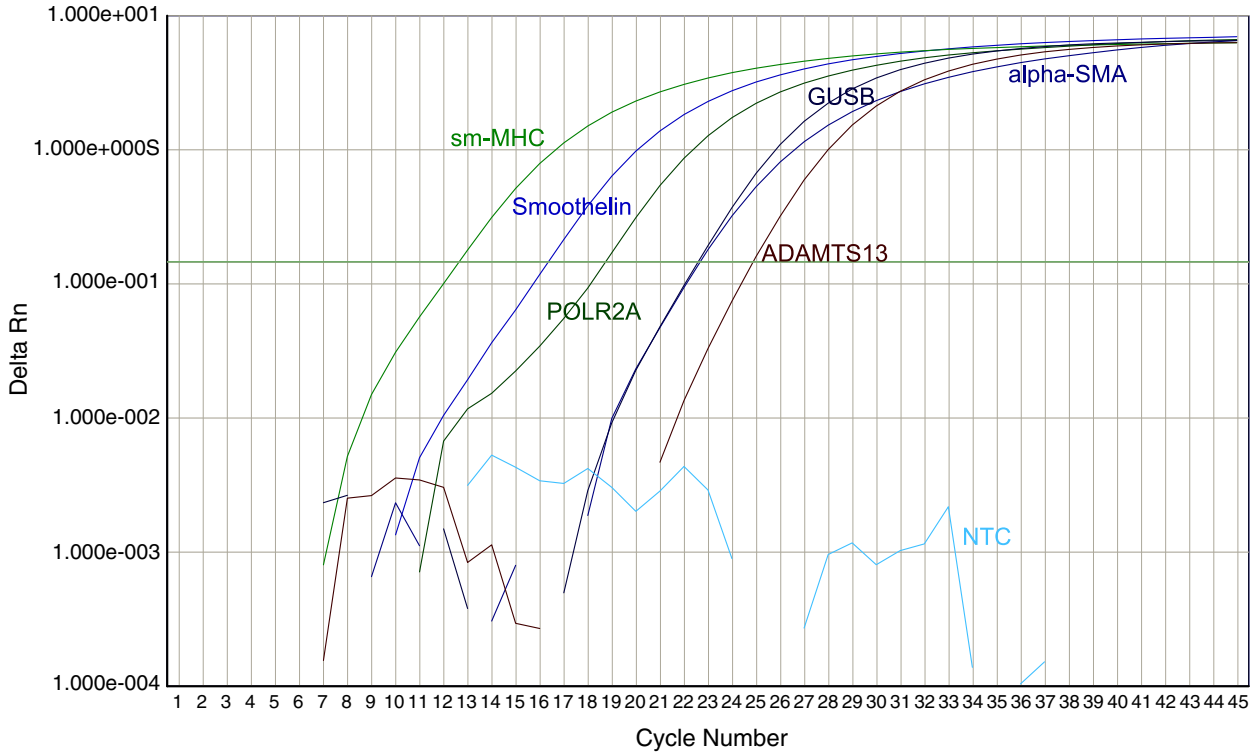

Fig. 2. Representative quantitative RT-PCR curves from the microdissected media of a hilar renal artery. ADAMTS13 mRNA is clearly detected. sm-MHC, smooth muscle myosin heavy chain; POLR2A, polymerase II, RNA, subunit A; GUSB, beta-glucuronidase; ADAMTS13, a disintegrin-like and metalloprotease with thrombospondin type-1 motif, 13; alpha-SMA, alpha-smooth muscle actin; NTC, non-template control.

(see Figure 1). Staining intensity was about equal in ECs and VSMCs and was as follows: aorta (2/3 moderate, 1/3 strong), renal artery (2/3 moderate, 1/3 strong, see Figure 1A), parenchymal arteries of spleen (2/3 moderate, 1/3 strong), kidney (5/7 moderate, 2/7 strong, see Figures 1B, 1C and 4D), placenta (3/3 moderate), pancreas (3/3 minimal), lung (1/3 minimal, 2/3 moderate), heart (1/3 minimal, 2/3 moderate), liver (3/3 minimal) and brain (3/3 moderate).

Quantitative RT-PCR of ADAMTS13, sm-MHC, alpha-SMA and smoothelin. Quantitative RT-PCR with RNA isolated from healthy arterial VSMCs confirmed the presence of ADAMTS13 mRNA in arterial VSMCs (see Figures 2 and 3). Relative expression levels of ADAMTS13 (0.06 ± 0.026) were lower than the levels of sm-MHC (317 ± 51.5), alpha-SMA (0.19 ± 0.055) and smoothelin (23 ± 3.6). The NTC gave consistent negative results (see example in Figure 2).

Human kidney specimens

Clinical data. Clinical data of the 54 specimens with bN and the 7 control specimens are given in Tables 2–5. Systolic blood pressure correlated significantly (P = 0.0051) with bN-grade, HScore (P = 0.0013) and FScore (P = 0.0093, see Tables 3–5). Diastolic blood pressure correlated with the presence or absence of bN (see Table 2), HScore (P = 0.0138, see Table 4) and FScore (P = 0.0498, see Table 5).

Serum creatinine correlated significantly with bN-grade (P = 0.0081, see Table 3), HScore (P = 0.0022, see Table 4) and FScore (P = 0.0083, see Table 5).

Conventional light microscopy and bN scoring. All seven normal renal control specimens had HScores and FScores of 0. Among the specimens with bN, the bN-grade had a distribution of 26/54 (48%) minimal, 20/54 (37%) moderate and 8/54 (15%) severe. The distribution of HScores and FScores among all specimens is given in Tables 4 and 5.

The mean frequency of globally sclerosed glomeruli is given in Tables 3–5. BN-grade and HScores did not correlate with the mean frequency of globally sclerosed glomeruli. However, the FScores did (P = 0.0123).

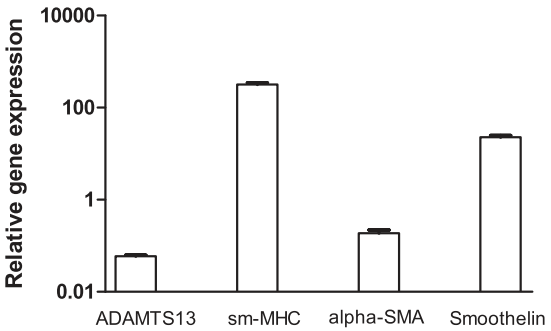

Fig. 3. ADAMTS13 mRNA is confirmed by quantitative RT-PCR in three VSMC samples microdissected from three formalin-fixed and paraffin-embedded hilar renal arteries. Relative gene expression levels are calculated in relation to the mean of reference genes POLR2A and GUSB as described in the Materials and methods section. Levels are shown as mean ± standard deviation.

Table 3. Clinicopathological parameters relative to the severity of bN (bN-grade)

	Absent bN $n = 7$	Minimal bN $n = 26$	Moderate bN $n = 20$	Severe bN $n = 8$
HScore 0	7/7 (100%)	1/26 (4%)	0/20 (0%)	0/8 (0%)
HScore 1	0/7 (0%)	22/26 (85%)	5/20 (25%)	0/8 (0%)
HScore 2	0/7 (0%)	3/26 (11%)	12/20 (60%)	1/8 (12%)
HScore 3	0/7 (0%)	0/26 (0%)	3/20 (15%)	7/8 (78%)
FScore 0	7/7 (100%)	13/26 (50%)	0/20 (0%)	0/8 (0%)
FScore 1	0/7 (0%)	13/26 (50%)	8/20 (40%)	0/8 (0%)
FScore 2	0/7 (0%)	0/26 (0%)	11/20 (55%)	4/8 (0%)
FScore 3	0/7 (0%)	0/26 (0%)	1/20 (5%)	4/8 (0%)
Systolic blood pressure (mm Hg)*	107 ± 14.7 ($n = 7$)	124 ± 20.0 ($n = 24$)	137 ± 33.3 ($n = 19$)	154 ± 18.9 ($n = 7$)
Diastolic blood pressure (mm Hg)	66 ± 9.2 ($n = 7$)	74 ± 10.3 ($n = 24$)	82 ± 22.4 ($n = 18$)	81 ± 14.6 ($n = 7$)
Serum creatinine (μmol/L)*	80 ± 22.5 ($n = 6$)	130 ± 63.9 ($n = 22$)	190 ± 130.0 ($n = 17$)	298 ± 176.0 ($n = 8$)
Global glomerulosclerosis	2.4 ± 6.3%	10.3 ± 17.7%	16.1 ± 20.9%	23.0 ± 24.4%
FSGS	0.0 ± 0.0%	0.2 ± 1.2%	3.4 ± 7.7%	3.1 ± 6.2%
IFTA 0*	7/7 (100%)	16/26 (61%)	8/20 (40%)	2/8 (24%)
IFTA 1*	0/7 (0%)	9/26 (35%)	7/20 (35%)	1/8 (13%)
IFTA 2*	0/7 (0%)	0/26 (0%)	2/20 (10%)	1/8 (13%)
IFTA 3*	0/7 (0%)	1/26 (4%)	3/20 (15%)	4/8 (50%)

HScore, hyalinosis score; FScore, fibrosis score; FSGS, focal segmental glomerulosclerosis; IFTA, score of interstitial fibrosis and tubular atrophy.
*$P < 0.05$.

Table 4. Clinicopathological parameters in relation to severity of hyalinosis (HScore)

	HScore 0 $n = 8$	HScore 1 $n = 27$	HScore 2 $n = 16$	HScore 3 $n = 10$
Systolic blood pressure (mm Hg)*	106 ± 13.8 ($n = 8$)	124 ± 24.2 ($n = 26$)	141 ± 24.7 ($n = 13$)	152 ± 27.4 ($n = 9$)
Diastolic blood pressure (mm Hg)*	66 ± 8.7 ($n = 8$)	72 ± 15.2 ($n = 26$)	84 ± 17.6 ($n = 14$)	84 ± 15.1 ($n = 9$)
Serum creatinine (μmol/L)*	80 ± 22.5 ($n = 6$)	142 ± 79.3 ($n = 24$)	154 ± 113.6 ($n = 13$)	308 ± 161.0 ($n = 10$)
Global glomerulosclerosis	3 ± 6.3% ($n = 8$)	11 ± 16.3% ($n = 27$)	14 ± 19.2% ($n = 16$)	24 ± 29.1 ($n = 10$)
FSGS	0 ± 0.0%	0 ± 1.1%	0 ± 7.9%	4.0 ± 6.8%
IFTA 0*	8/8 (100%)	15/27 (56%)	7/16 (44%)	3/10 (30%)
IFTA 1*	0/8 (0%)	10/27 (37%)	6/16 (38%)	1/10 (10%)
IFTA 2*	0/8 (0%)	0/27 (0%)	2/16 (12%)	1/10 (10%)
IFTA 3*	0/8 (0%)	2/27 (7%)	1/16 (6%)	5/10 (50%)

HScore, hyalinosis score; FScore, fibrosis score; FSGS, focal segmental glomerulosclerosis; IFTA, score of interstitial fibrosis and tubular atrophy.
*$P < 0.05$.

Table 5. Clinicopathological parameters in relation to severity of arteriolar fibrosis (FScore)

	FScore 0 $n = 20$	FScore 1 $n = 21$	FScore 2 $n = 15$	FScore 3 $n = 5$
Systolic blood pressure (mm Hg)*	115 ± 17.0 ($n = 19$)	132 ± 26.4 ($n = 20$)	138 ± 32.7 ($n = 12$)	157 ± 21.2 ($n = 5$)
Diastolic blood pressure (mm Hg)*	69 ± 10.3 ($n = 19$)	78 ± 12.0 ($n = 20$)	80 ± 25.2 ($n = 12$)	88 ± 16.8 ($n = 5$)
Serum creatinine (μmol/L)*	105 ± 41.0 ($n = 18$)	160 ± 96.5 ($n = 18$)	195 ± 143.0 ($n = 12$)	370 ± 158.1 ($n = 5$)
Global glomerulosclerosis*	8 ± 15.7% ($n = 20$)	11 ± 20.5% ($n = 21$)	14 ± 15.9% ($n = 15$)	40 ± 20.0% ($n = 5$)
FSGS	0 ± 1.3% ($n = 20$)	3 ± 7.1 ($n = 21$)	2 ± 4.1% ($n = 15$)	3 ± 7.5% ($n = 5$)
IFTA 0*	16/20 (80%)	10/21 (48%)	7/15 (47%)	0/5 (0%)
IFTA 1*	4/20 (20%)	9/21 (43%)	3/15 (20%)	1/5 (20%)
IFTA 2*	0/20 (0%)	0/21 (0%)	3/15 (20%)	0/5 (0%)
IFTA 3*	0/20 (0%)	2/21 (9%)	2/15 (13%)	4/5 (80%)

HScore, hyalinosis score; FScore, fibrosis score; FSGS, focal segmental glomerulosclerosis; IFTA, score of interstitial fibrosis and tubular atrophy.
*$P < 0.05$.

FSGS was present in 7/54 patients (13%) with bN. FSGS type was perihilar in one specimen with a minimal bN-grade, three with a moderate and one with a severe bN-grade. One single case of FSGS NOS each was present among the patients with moderate and severe bN. The distribution of the frequency of focally and segmentally sclerotic glomeruli is given in Tables 3–5. FSGS was not observed in the control specimens without bN.

The severity score of cortical IFTA also correlated significantly with bN-grade ($P = 0.0062$, see Table 3), HScore ($P = 0.0020$, see Table 4) and FScore ($P < 0.0001$, see Table 5).

Thrombi were found in none of the specimens.

ADAMTS13 immunohistochemistry. Representative examples are depicted in Figure 4D–F, and a comprehensive overview of the results is given in Figure 5A–C. Results

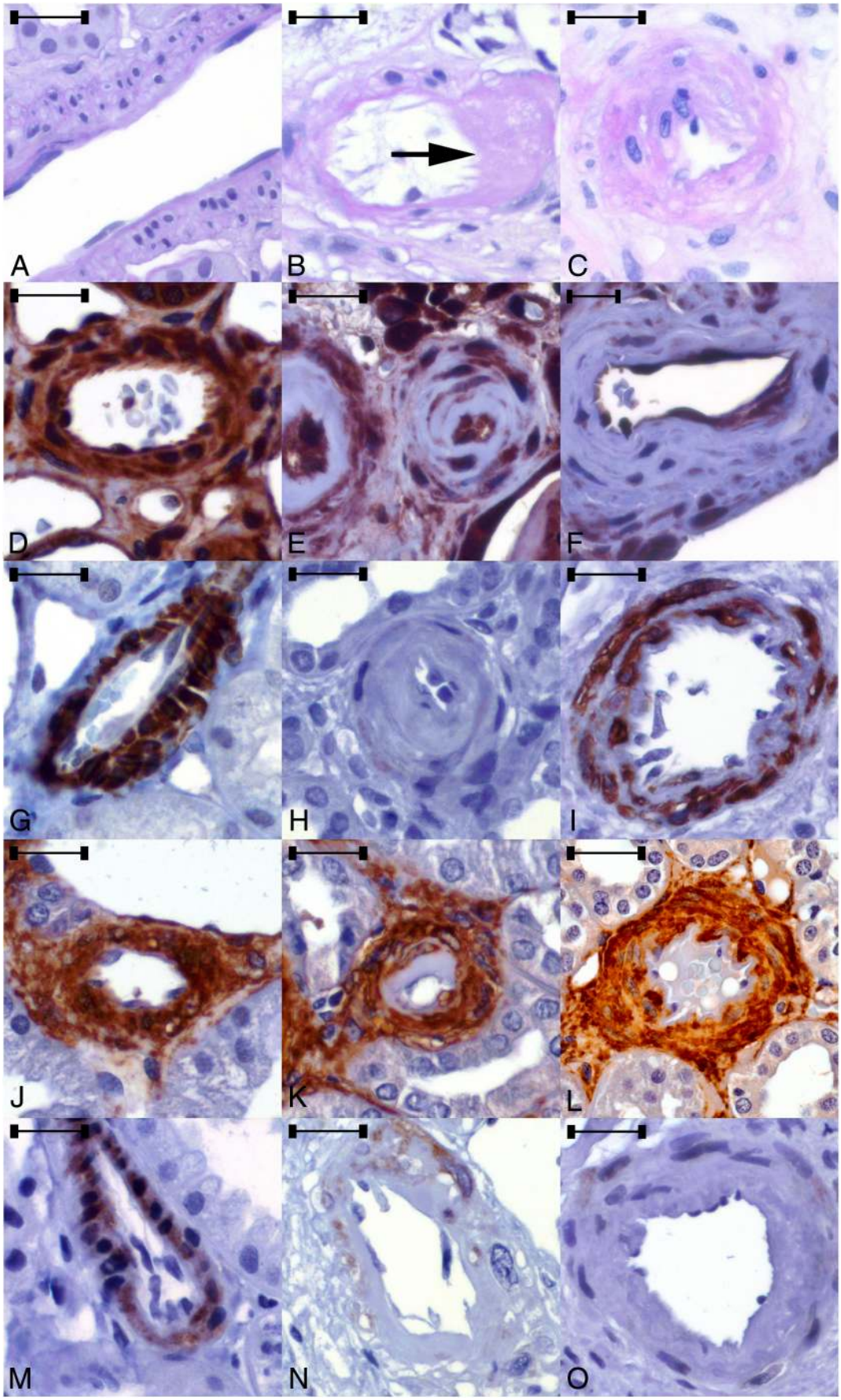

of ADAMTS13 immunostaining of VSMCs in small preglomerular vessels correlated inversely with bN-grades ($P = 0.0422$, Figure 5A). ADAMTS13 staining of these vessels did not correlate with HScore (see Figure 5B), but correlated inversely with FScores ($P = 0.0060$, Figure 5C).

sm-MHC immunohistochemistry. sm-MHC was positive only in VSMCs in a diffuse cytoplasmic pattern (representative micrographs in Figure 4G–I). sm-MHC immunostaining did not show any correlation with bN-grade (see Figure 5D). sm-MHC staining in VSMCs of small preglomerular vessels correlated inversely with HScores ($P = 0.0111$, see Figure 5E), but did not correlate with FScores (see Figure 5F).

Alpha-SMA immunohistochemistry. Alpha-SMA was positive in VSMCs in a diffuse cytoplasmic pattern in all specimens (representative micrographs given in Figure 4J–L). Immunostaining of VSMCs of small preglomerular vessels did not correlate with bN-grade, FScore or HScore (see Figure 5G–I).

Smoothelin immunohistochemistry. Smoothelin was present in the VSMCs of small preglomerular vessels in a diffuse cytoplasmic pattern also (see Figure 4M–O). The intensity of the immunostaining correlated inversely with bN-grade ($P < 0.0001$, see Table 5J), HScore ($P = 0.0001$, see Table 5K) and FScore ($P = 0.0119$, see Table 5L).

Additional immunohistochemistry for VWF and CD61. In order to evaluate the pathophysiological role of ADAMTS13 in bN, all samples were immunostained for activated platelets and VWF. No CD61-positive cells were detected in the subendothelial parts of small preglomerular vessels (see Figure 6) in any of the 54 bN specimens and 7 controls. None of the six control specimens without bN that could be evaluated for VWF immunostaining were positive in the subendothelial space. In contrast, 7/54 (13%) specimens with bN were positive for VWF in the subendothelial space. Notably all hyalinotic lesions were negative for VWF (see Figure 6).

Discussion

Regulatory proteins of the coagulation system, for example plasminogen activator inhibitor-1, are expressed not only by ECs but also by VSMCs deeper in the arterial wall [5,21,25]. Another example is tissue factor, which can rapidly be induced by injury in arterial VSMCs [28].

The present manuscript adds ADAMTS13 to this list. ADAMTS13 expression has already been confirmed in hepatic stellate cells [47,53] and podocytes [37], both of which are closely related to VSMCs. ADAMTS13 seems to be expressed in VSMCs at an almost equal level throughout the arterial system, in arteries of elastic and muscular type and also in small preglomerular vessels in the kidney. Other members of the ADAMTS family have also been reported in VSMCs. ADAMTS1 has been found in VSMCs of developing mice [41] and also in humans [19]. ADAMTS7 is present in VSMCs of rat carotid arteries and promotes VSMC migration and neointima formation [49].

With the present results, we can only speculate what the (patho-)physiological role of ADAMTS13 expression in VSMCs might be. VWF, the only known substrate of ADAMTS13, is known to be secreted by ECs in arteries not only into the lumen but also into the subendothelial space [36].

Our results support this notion (see Figure 6C). VWF multimers are known to induce intimal fibrosis and VSMC proliferation [33]. It is thus conceivable that ADAMTS13 might cleave and degrade VWF multimers that have permeated into the arterial wall. Since the hyalin deposits in preglomerular vessel walls are thought to consist of plasma insudation through leaky endothelium into the vessel wall [11,15–17], we speculated that this hyaline contained VWF and possibly also platelets. Together they might initiate fibrosis of the vessel wall in hypertension.

Surprisingly, neither VWF nor activated platelets could be found by immunohistochemistry in the hyaline deposits (see Figure 6A–D). Consequently, the hypothesis that diminished production of ADAMTS13 could lead to a procoagulant and thus profibrotic micromilieu via accumulation of ultralarge VWF multimers and activated platelets in the arterial wall is probably incorrect—incorrect at least in the early hyalinotic stage of bN, in which ADAMTS13 immunostaining was preserved. Nevertheless, 13% of the specimens with bN lesions showed VWF immunostaining in the subendothelial compartment of the arteriolar walls exclusively in fibrotic, but not in hyalinotic, lesions, while the normal controls were consistently negative. FScores correlated significantly with decreased immunostaining of VSMCs for VWF cleaving protease ADAMTS13. Taken together, these findings support the hypothesis that a disturbed balance between accumulating VWF multimers and diminished ADAMTS13 might further propagate fibrosis in the later lesions of bN.

Fig. 4. Immunostaining of arteriolar VSMCs in human kidneys without and with hyalinotic and fibrotic lesions of benign nephrosclerosis (bN): (**A**) normal arteriole, (**B**) hyalinosis in the arteriolar wall segment to the right (arrow) and (**C**) fibrotic lesions with multilamellated appearance (all periodic acid Schiff (PAS) stain, original magnification ×600, scale bar 25 μm). (**D**) Strong ADAMTS13 immunostaining (brown) in vascular smooth muscle cells (VSMCs) and endothelial cells (ECs) of a normal arteriole, (**E**) strong ADAMTS13 immunostaining of VSMCs in two hyalinotic arterioles, (**F**) minimal ADAMTS13 immunostaining of VSMCs in fibrotic bN (all immunoperoxidase, original magnification in D and E ×600, scale bar 25 μm; original magnification in F ×400, scale bar 25 μm). (**G**) Strong sm-MHC immunostaining (brown) in VSMCs of normal arteriole, (**H**) absent sm-MHC immunostaining of VSMCs in hyalinotic arteriole, (**I**) strong sm-MHC immunostaining of VSMCs in fibrotic lesion of bN (all immunoperoxidase, original magnification ×600, scale bar 25 μm). (**J**) Moderate alpha-SMA immunostaining (brown) in vascular VSMCs of normal arteriole, (**K**) moderate alpha-SMA immunostaining of VSMCs in hyalinotic bN, (**L**) moderate alpha-SMA immunostaining of VSMCs in fibrotic lesion of bN (all immunoperoxidase, original magnification ×600, scale bar 25 μm). (**M**) Moderate smoothelin immunostaining (brown) in VSMCs of normal arteriole, (**N**) minimal smoothelin immunostaining of VSMCs in hyalinotic bN, (**O**) minimal smoothelin immunostaining of VSMCs in fibrotic bN (all immunoperoxidase, original magnification ×600, scale bar 25 μm).

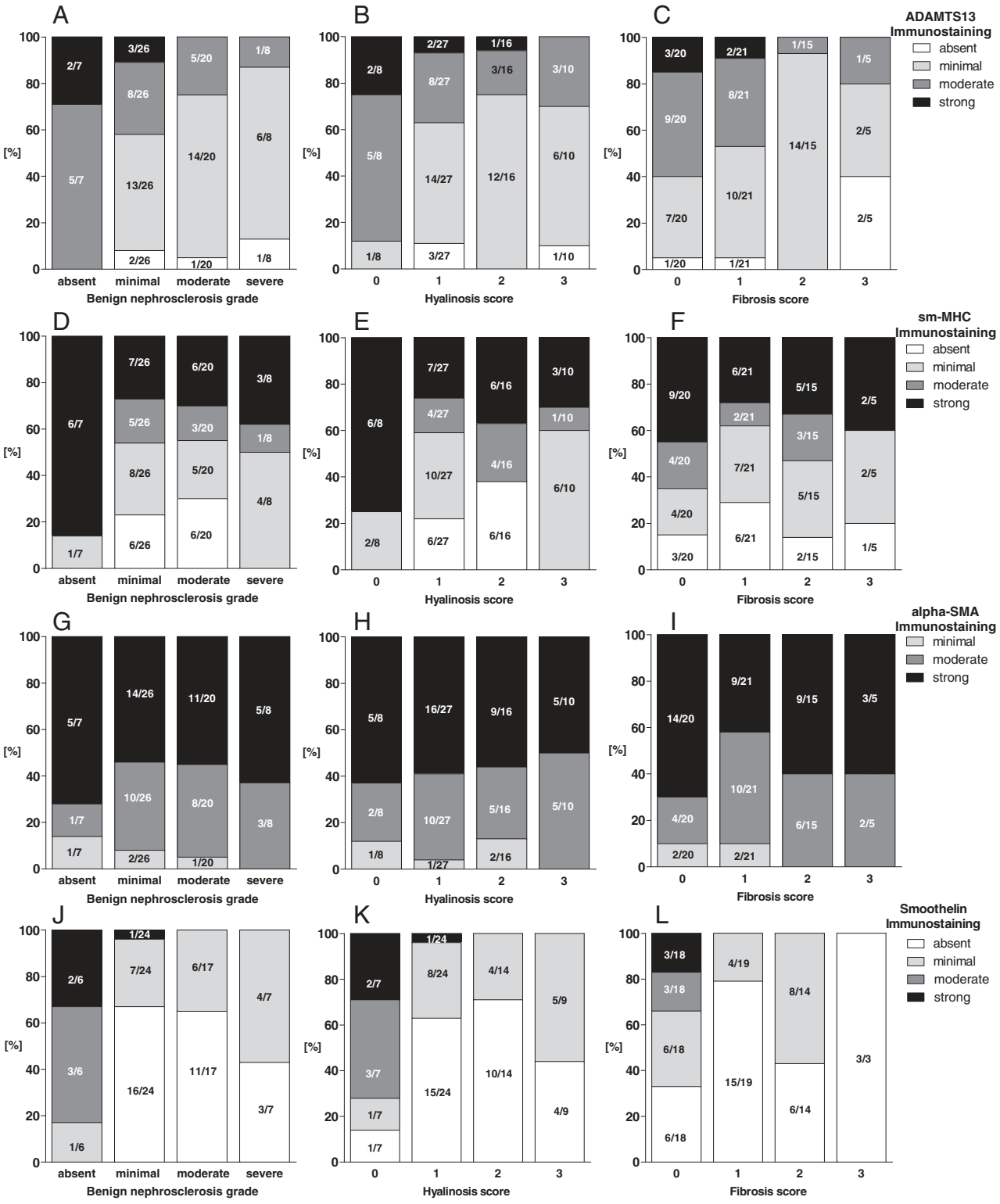

Fig. 5. Comprehensive results of ADAMTS13, sm-MHC, alpha-SMA and smoothelin immunostaining of arteriolar VSMCs. HScore, hyalinosis score; FScore, fibrosis score.

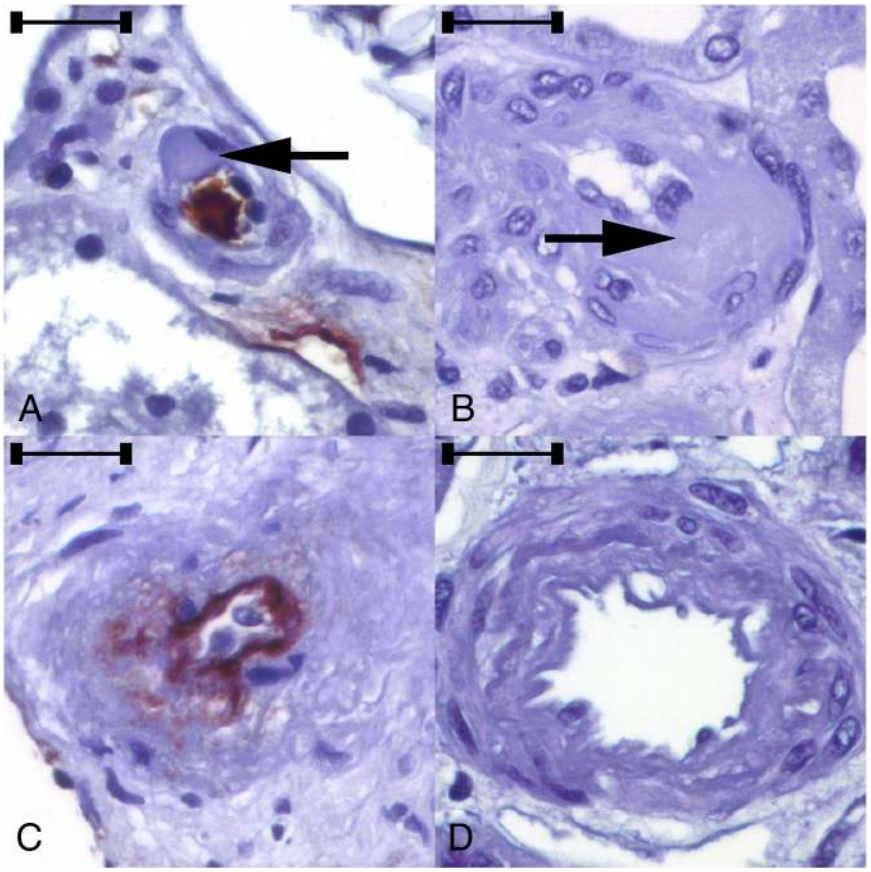

Fig. 6. VWF and CD61 immunostaining of arteriolar walls with hyalinotic and fibrotic lesions of benign nephrosclerosis: (**A**) only endothelium positive for VWF (brown), hyalinosis (arrow) negative. VWF immunoperoxidase, original magnification ×600, scale bar 50 μm. (**B**) No activated platelets within the entire arteriolar wall including hyalinosis (arrow). CD61 immunoperoxidase, original magnification ×600, scale bar 50 μm. (**C**) Leakage of VWF (brown) from the positive endothelium into the fibrotic arteriolar wall. VWF immunoperoxidase, original magnification ×600, scale bar 50 μm. (**D**) No activated platelets within the entire fibrotic arteriolar wall. CD61 immunoperoxidase, original magnification ×600, scale bar 50 μm.

VSMCs can acquire contractile or secretory phenotypes [24]. The normal phenotype of VSMCs is contractile, while the secretory phenotype is considered pathologic and contributory to lesions such as atherosclerosis [4,24,35]. It is conceivable that VSMCs of small preglomerular vessels lose their normal contractile phenotype and acquire a secretory phenotype in the progression from normal via hyalinotic to fibrotic lesions of bN. Several marker proteins are known to be characteristic for the normal contractile phenotype, of which we examined alpha-SMA, sm-MHC and smoothelin.

Markers that are upregulated in the secretory phenotype are rare, and therefore, this phenotype is generally characterized by the absence of contractile markers [34]. The finding that ADAMTS13 staining is inversely correlated with overall scores of bN and fibrotic type bN, but not with hyalinotic lesions of bN, indicates that ADAMTS13 could be a novel marker of the contractile phenotype of arteriolar VSMCs that is kept in hyalinotic but lost in fibrotic lesions of bN when VSMCs dedifferentiate towards a secretory phenotype and the secreted collagen has already accumulated. Comparison with the established markers of contractile phenotype alpha-SMA [9,18] and sm-MHC [14] showed that alpha-SMA correlated neither with HScores, FScores, now with bN-grade. Consequently, alpha-SMA seems to be an inferior marker of arteriolar VSMC differentiation. Interestingly, analysis of the sm-MHC immunostaining pattern of VSMCs of small preglomerular vessels (see Figure 1G) showed an inverse correlation with HScores but no correlation with FScore or bN-grade. This suggests that sm-MHC could be a marker of acute dedifferentiation in early hyalinotic lesions of bN, which is regained in the chronic, irreversible fibrotic lesions of bN. In this respect, sm-MHC seems to be a complementary marker to ADAMTS13, the loss of which indicates chronic, fibrotic damage. The polyclonal antibody that was used for smoothelin immunostaining recognizes both A and B isoforms. The shorter A isoform is only present in smooth muscle cells of the intestinal muscularis propria [22]. The longer B isoform is only expressed in VSMCs [48]. Smoothelin immunostaining correlated inversely with the severity of both hyalinotic and fibrotic lesions of bN. Therefore, smoothelin is probably the most sensitive marker of the contractile phenotype, with diminished immunostaining even in early, hyalinotic lesions of bN. In this regard, it is superior to ADAMTS13 because diminished smoothelin immunostaining seems to indicate even minor and acute damage to arteriolar VSMCs in bN.

Loss of ADAMTS13 expression in arteriolar VSMCs could also have a direct role in extracellular matrix (ECM) accumulation. It has been speculated that ADAMTS13, as a metalloprotease, might also be involved in ECM degradation [26]. ECM accumulation through diminished degradation in fibrotic lesions of bN with partial loss of ADAMTS13 expression in VSMCs could be a novel pathomechanism in the development of bN. Further insight into additional functions of ADAMTS13 in health and disease could be gained from examination of patients with congenital defects in ADAMTS13 (Upshaw–Schulman syndrome) or from ADAMTS13-knockout mice. Unfortunately, all renal biopsies in our archives from Upshaw–Schulman patients showed severe changes of thrombotic microangiopathy with concomitant malignant nephrosclerosis. No further renal or extrarenal tissue samples could be allocated through inquiries at major German paediatric centres. We are also not aware of any detailed histomorphological description of vessel walls in 'healthy' or hypertensive ADAMTS13-knockout mice.

Therefore, it seems premature to ascribe ADAMTS13 a definitive role in ECM degradation, as substrates of ADAMTS13 other than VWF multimers have yet to be established.

A recently published manuscript by Taniguchi *et al.* links diabetic macroangiopathy and renal diabetic microangiopathy to reduced serum levels of ADAMTS13 [40]. Intravascular ADAMTS13, as measured in the serum, is probably mainly derived from the vascular endothelium as our immunohistochemical stains support (see Figure 1). Endothelial dysfunction in diabetes could lead to decreased secretion of ADAMTS13. Diminished intravascular levels of ADAMTS13 could then cause microthrombi in the intravascular compartment. Indeed, glomerular microthrombi have been reported in a substantial number of biopsies with diabetic glomerulopathy [31]. In contrast to Taniguchi's work, the present manuscript addresses ADAMTS13 expressed by VSMCs. ADAMTS13 derived from VSMCs probably remains in the media and therefore should not contribute significantly to serum levels of ADAMTS13 and should have no antithrombotic effects within the intravascular compartment. In support of this, we did not observe any intravascular thrombi nor are there any literature reports of thrombi in bN known to us. Nevertheless, additional studies could potentially clarify whether ADAMTS13 serum levels are diminished in patients with bN.

Conclusion

In summary, it is proven for the first time that ADAMTS13 is expressed in arterial and arteriolar VSMCs throughout the human organism. The role of ADAMTS13 expression in VSMCs is probably cleavage of endothelium-derived VWF multimers permeating into the arterial walls. ADAMTS13 can be considered a marker of the contractile phenotype that is lost in the chronic, fibrotic lesions of bN. Loss of ADAMTS13 and accumulation of VWF exclusively in fibrotic arteriolar lesions could contribute to fibrosis propagation in bN.

Acknowledgements. The authors would like to thank Ulrich O. Wenzel for helpful discussions and review of the manuscript, Gillian Theike for careful English proofreading and the nephrologists from Hannover, Bremen, Minden and Offenbach for providing additional clinical data.

Conflict of interest statement. No conflict of interest.

(See related article by Amann. ADAMTS13—more than just TMA and TTP. *Nephrol Dial Transplant* 2011; 26: 1761–1764)

References

1. Annual Data Report 2009: Volume Two: Atlas of End-Stage Renal Disease. United States Renal Database, 2009
2. *WMA Declaration of Helsinki - Ethical Principles for Medical Research Involving Human Subjects*. Helsinki: World Medical Association, 2008
3. Anstee QM, Goldin RD, Wright M *et al*. Coagulation status modulates murine hepatic fibrogenesis: implications for the development of novel therapies. *J Thromb Haemost* 2008; 6: 1336–1343
4. Campbell GR, Campbell JH. Smooth muscle phenotypic changes in arterial wall homeostasis: implications for the pathogenesis of atherosclerosis. *Exp Mol Pathol* 1985; 42: 139–162
5. Chomiki N, Henry M, Alessi MC *et al*. Plasminogen activator inhibitor-1 expression in human liver and healthy or atherosclerotic vessel walls. *Thromb Haemost* 1994; 72: 44–53
6. D'Agati VD, Fogo AB, Bruijn JA *et al*. Pathologic classification of focal segmental glomerulosclerosis: a working proposal. *Am J Kidney Dis* 2004; 43: 368–382
7. Fogo AB. Mechanisms of progression of chronic kidney disease. *Pediatr Nephrol* 2007; 22: 2011–2022
8. Freedman BI, Iskander SS, Buckalew VMJr *et al*. Renal biopsy findings in presumed hypertensive nephrosclerosis. *Am J Nephrol* 1994; 14: 90–94
9. Frid MG, Shekhonin BV, Koteliansky VE *et al*. Phenotypic changes of human smooth muscle cells during development: late expression of heavy caldesmon and calponin. *Dev Biol* 1992; 153: 185–193
10. Furlan M, Robles R, Solenthaler M *et al*. Acquired deficiency of von Willebrand factor-cleaving protease in a patient with thrombotic thrombocytopenic purpura. *Blood* 1998; 91: 2839–2846
11. Gamble CN. The pathogenesis of hyaline arteriolosclerosis. *Am J Pathol* 1986; 122: 410–420
12. Griffin KA, Bidani AK. Hypertensive renal damage: insights from animal models and clinical relevance. *Curr Hypertens Rep* 2004; 6: 145–153
13. Griffin KA, Kramer H, Bidani AK. Adverse renal consequences of obesity. *Am J Physiol Renal Physiol* 2008; 294: F685–F696
14. Halayko AJ, Salari H, Ma X *et al*. Markers of airway smooth muscle cell phenotype. *Am J Physiol* 1996; 270: L1040–L1051
15. Helmchen U, Wenzel UO. Renal Pathology with Clinical and Functional Correlations. In: CC Tisher, BM Brenner (eds). Philadelphia: JB Lippincott Company, 1994
16. Hill GS, Heudes D, Bariety J. Morphometric study of arterioles and glomeruli in the aging kidney suggests focal loss of autoregulation. *Kidney Int* 2003; 63: 1027–1036
17. Hill GS, Heudes D, Jacquot C *et al*. Morphometric evidence for impairment of renal autoregulation in advanced essential hypertension. *Kidney Int* 2006; 69: 823–831
18. Hungerford JE, Owens GK, Argraves WS *et al*. Development of the aortic vessel wall as defined by vascular smooth muscle and extracellular matrix markers. *Dev Biol* 1996; 178: 375–392
19. Jonsson-Rylander AC, Nilsson T, Fritsche-Danielson R *et al*. Role of ADAMTS-1 in atherosclerosis: remodeling of carotid artery, immunohistochemistry, and proteolysis of versican. *Arterioscler Thromb Vasc Biol* 2005; 25: 180–185
20. Katafuchi R, Takebayashi S. Morphometrical and functional correlations in benign nephrosclerosis. *Clin Nephrol* 1987; 28: 238–243
21. Kouri FM, Queisser MA, Konigshoff M *et al*. Plasminogen activator inhibitor type 1 inhibits smooth muscle cell proliferation in pulmonary arterial hypertension. *Int J Biochem Cell Biol* 2008; 40: 1872–1882

22. Kramer J, Aguirre-Arteta AM, Thiel C *et al*. A novel isoform of the smooth muscle cell differentiation marker smoothelin. *J Mol Med* 1999; 77: 294–298
23. Levy GG, Nichols WC, Lian EC *et al*. Mutations in a member of the ADAMTS gene family cause thrombotic thrombocytopenic purpura. *Nature* 2001; 413: 488–494
24. Lindop GB, Boyle JJ, McEwan P *et al*. Vascular structure, smooth muscle cell phenotype and growth in hypertension. *J Hum Hypertens* 1995; 9: 475–478
25. Lupu F, Bergonzelli GE, Heim DA *et al*. Localization and production of plasminogen activator inhibitor-1 in human healthy and atherosclerotic arteries. *Arterioscler Thromb* 1993; 13: 1090–1100
26. Manea M, Kristoffersson A, Schneppenheim R *et al*. Podocytes express ADAMTS13 in normal renal cortex and in patients with thrombotic thrombocytopenic purpura. *Br J Haematol* 2007; 138: 651–662
27. Manea M, Tati R, Karlsson J *et al*. Biologically active ADAMTS13 is expressed in renal tubular epithelial cells. *Pediatr Nephrol* 2009; 25: 87–96
28. Marmur JD, Rossikhina M, Guha A *et al*. Tissue factor is rapidly induced in arterial smooth muscle after balloon injury. *J Clin Invest* 1993; 91: 2253–2259
29. Matsumoto M, Kokame K, Soejima K *et al*. Molecular characterization of ADAMTS13 gene mutations in Japanese patients with Upshaw-Schulman syndrome. *Blood* 2004; 103: 1305–1310
30. Mogensen CE. Twelve shifting paradigms in diabetic renal disease and hypertension. *Diabetes Res Clin Pract* 2008; 82 (Suppl 1): S2–S9
31. Paueksakon P, Revelo MP, Ma LJ *et al*. Microangiopathic injury and augmented PAI-1 in human diabetic nephropathy. *Kidney Int* 2002; 61: 2142–2148
32. Plaimauer B, Zimmermann K, Volkel D *et al*. Cloning, expression, and functional characterization of the von Willebrand factor-cleaving protease (ADAMTS13). *Blood* 2002; 100: 3626–3632
33. Qin F, Impeduglia T, Schaffer P *et al*. Overexpression of von Willebrand factor is an independent risk factor for pathogenesis of intimal hyperplasia: preliminary studies. *J Vasc Surg* 2003; 37: 433–439
34. Rensen SS, Doevendans PA, van Eys GJ. Regulation and characteristics of vascular smooth muscle cell phenotypic diversity. *Neth Heart J* 2007; 15: 100–108
35. Ross R. The pathogenesis of atherosclerosis–an update. *N Engl J Med* 1986; 314: 488–500
36. Ruggeri ZM. The role of von Willebrand factor in thrombus formation. *Thromb Res* 2007; 120Suppl 1S5–S9
37. Saleem MA, Zavadil J, Bailly M *et al*. The molecular and functional phenotype of glomerular podocytes reveals key features of contractile smooth muscle cells. *Am J Physiol Renal Physiol* 2008; 295: F959–F970
38. Sancho A, Gavela E, Avila A *et al*. Risk factors and prognosis for proteinuria in renal transplant recipients. *Transplant Proc* 2007; 39: 2145–2147
39. Schneppenheim R, Budde U, Oyen F *et al*. von Willebrand factor cleaving protease and ADAMTS13 mutations in childhood TTP. *Blood* 2003; 101: 1845–1850
40. Taniguchi S, Hashiguchi T, Ono T *et al*. Association between reduced ADAMTS13 and diabetic nephropathy. *Thromb Res* 2010; 125: e310–e316
41. Thai SN, Iruela-Arispe ML. Expression of ADAMTS1 during murine development. *Mech Dev* 2002; 115: 181–185
42. Theophile K, Hussein K, Kreipe H *et al*. Expression profiling of apoptosis-related genes in megakaryocytes: BNIP3 is downregulated in primary myelofibrosis. *Exp Hematol* 2008; 36: 1728–1738
43. Theophile K, Jonigk D, Kreipe H *et al*. Amplification of mRNA from laser-microdissected single or clustered cells in formalin-fixed and paraffin-embedded tissues for application in quantitative real-time PCR. *Diagn Mol Pathol* 2008; 17: 101–106
44. Tsai HM, Lian EC. Antibodies to von Willebrand factor-cleaving protease in acute thrombotic thrombocytopenic purpura. *N Engl J Med* 1998; 339: 1585–1594
45. Turner N, Nolasco L, Tao Z *et al*. Human endothelial cells synthesize and release ADAMTS-13. *J Thromb Haemost* 2006; 4: 1396–1404
46. Uemura M, Fujimura Y, Ko S *et al*. Pivotal role of ADAMTS13 function in liver diseases. *Int J Hematol* 91: 20–29
47. Uemura M, Tatsumi K, Matsumoto M *et al*. Localization of ADAMTS13 to the stellate cells of human liver. *Blood* 2005; 106: 922–924
48. van Eys GJ, Voller MC, Timmer ED *et al*. Smoothelin expression characteristics: development of a smooth muscle cell in vitro system and identification of a vascular variant. *Cell Struct Funct* 1997; 22: 65–72
49. Wang L, Zheng J, Bai X *et al*. ADAMTS-7 mediates vascular smooth muscle cell migration and neointima formation in balloon-injured rat arteries. *Circ Res* 2009; 104: 688–698
50. Wanless IR, Liu JJ, Butany J. Role of thrombosis in the pathogenesis of congestive hepatic fibrosis (cardiac cirrhosis). *Hepatology* 1995; 21: 1232–1237
51. Wirz W, Antoine M, Tag CG *et al*. Hepatic stellate cells display a functional vascular smooth muscle cell phenotype in a three-dimensional co-culture model with endothelial cells. *Differentiation* 2008; 76: 784–794
52. Wright M, Goldin R, Hellier S *et al*. Factor V Leiden polymorphism and the rate of fibrosis development in chronic hepatitis C virus infection. *Gut* 2003; 52: 1206–1210
53. Zhou W, Inada M, Lee TP *et al*. ADAMTS13 is expressed in hepatic stellate cells. *Lab Invest* 2005; 85: 780–788

Received for publication: 14.4.10; Accepted in revised form: 9.9.10